MENU 2007
11th International Conference
on Meson-Nucleon Physics and
the Structure of the Nucleon
September10-14, 2007
IKP, Forschungzentrum Jülich, Germany

K^+ PHOTOPRODUCTION AND π^0 PHOTOPRODUCTION BY LINEARLY POLARIZED PHOTONS AT SPring-8/LEPS

M.Sumihama[⋆,1], J.K. Ahn[%], H. Akimune[#], Y. Asano[⊔], W.C. Chang[$], S. Daté[⊔], H. Ejiri[⊔], H. Fujimura[&], M. Fujiwara[⋆], K. Hicks[+], T. Hotta[⋆], K. Imai[&], T. Ishikawa[±], T. Iwata[∓], H. Kawai[×], K. Kino[⋆], H. Kohri[⋆], N. Kumagai[⊔], S. Makino[⊗], T. Matsumura[⋆], N. Matsuoka[⋆], T. Mibe[+], M. Miyabe[&], M. Morita[⋆], N. Muramatsu[⋆], T. Nakano[⋆], M. Niiyama[&], M. Nomachi[°], Y. Ohashi[⊔], H. Ohkuma[⊔], T. Ooba[×], D.S. Oshuev[$], C. Rangacharyulu[•], A. Sakaguchi[°], T. Sato[°], P.M. Shagin[÷], Y. Shiino[×], H. Shimizu[±], Y. Sugaya[°], H. Toyokawa[⊔], C.W. Wang[$], S.C. Wang[$], K. Yonehara[#], T. Yorita[⋆], M. Yosoi[⋆], R.G.T. Zegers[∪]

[⋆] Research Center for Nuclear Physics, Osaka University, Ibaraki, Japan
[%]Department of Physics, Pusan National University, Busan, Korea
[#]Department of Physics, Konan University, Kobe, Japan
[⊔]Japan Synchrotron Radiation Research Institute,Sayo, Hyogo, Japan
[$]Institute of Physics, Academia Sinica, Taipei, Taiwan
[&]Department of Physics, Kyoto University, Kyoto, Japan
[+]Department of Physics and Astronomy, Ohio University, Athens, Ohio, USA
[±]Laboratory of Nuclear Science, Tohoku University, Sendai, Japan
[∓]Department of Physics, Yamagata University, Yamagata, Japan
[×]Graduate School of Science and Technology, Chiba University, Chiba, Japan
[⊗]Wakayama Medical College, Wakayama, Japan
[°]Department of Physics, Osaka University, Toyonaka, Japan
[•]Department of Physics and Engineering Physics, University of Saskatchewan, Saskatoon, Saskatchewan, Canada
[÷]School of Physics and Astronomy, University of Minnesota, Minneapolis, Minnesota
[∪]National Superconducting Cyclotron Laboratory, Michigan State University, Michigan, USA

Abstract

K^+ photoproduction and π^0 photoproduction have been measured by linearly polarized photons from 1.5 GeV to 2.4 GeV at the SPring-8/LEPS facility. Differential cross sections and photon beam asymmetries for the $\gamma p \to K^+\Lambda$, $\gamma p \to K^+\Sigma^0$, and $\gamma p \to p\pi^0$ reactions have been obtained.

[1]E-mail address: sumihama@rcnp.osaka-u.ac.jp

1 Introduction

The spectroscopy of N* and Δ* resonances has been studied both experimentally and theoretically. Many baryon resonances were found and their characteristics were determined at the total energy, $W < 1.7$ GeV [**?**]. However many higher-mass resonances are still not well established, which are called "missing resonances" [1, 2]. A huge number of baryon resonances are predicted in the constituent quark models, but only a part of these expected resonances is experimentally observed [2]. Identification of the missing resonances is important to understand the quark-gluon structure of a nucleon.

Quark model studies suggest some of these missing resonances may couple to strange channels, such as $K\Lambda$ and $K\Sigma$ channels [2]. Λ and Σ^0 hyperons have the isospins of 0 and 1, respectively. Accordingly, intermediate states of $K^+\Lambda$ have the isospin $\frac{1}{2}$ whereas intermediate states of $K^+\Sigma^0$ can have both the isospins of $\frac{1}{2}$ and $\frac{3}{2}$. It is very interesting to study the $\gamma p \to K^+\Lambda$ and $\gamma p \to K^+\Sigma^0$ reactions to further our understanding of the role that nucleon resonances play in non-pionic reactions.

Valuable information on baryon resonances has been obtained primarily from the studies of pion channels. There still remains a possibility to obtain new information on baryon resonances in pion photoproduction by measuring polarization observables at high energies. Some weakly excited resonances are obscured due to other strong resonances which have large decay widths, making it difficult to demonstrate their existence only from the cross section data. Alternatively, polarization observables are useful to extract such hidden resonances [3].

At very forward (backward) angles, the production mechanism is expected to be dominated by t-channel (u-channel) contributions. In general, differential cross sections of meson photoproduction are well described using a simple equation of $s^{2\alpha(t)-2}$ ($s^{2\alpha(u)-2}$) on basis of the Regge theory at high energies $E_\gamma > 3$ GeV [4, 5]. Unfortunately, the applicability of Regge theory is not well demonstrated at lower energies due to the lack of experimental data at backward angles. Such experimental data are obtained at the LEPS facility with photons at E_γ =1.5 – 2.4 GeV, and provide a good means to understand the reaction mechanism. We measured K^+ photoproduction in t-channel kinematics, and π^0 photoproduction in u-channel kinematics.

2 Experiment

The experiment was carried out at the Laser-Electron-Photon beam line of the Super Photon ring 8-GeV facility (SPring-8/LEPS) [6, 7]. A multi-

GeV photon beam was produced by backward-Compton scattering (BCS) between Ar-ion laser photons with a 351-nm wave length and the circulating 8-GeV electrons in the storage ring. The linearly polarized photon beam was obtained from the BCS process with linearly-polarized laser photons. The polarization of the photon beam was about 95% at the maximum energy, 2.4 GeV and about 55% at the lowest energy, 1.5 GeV. The photon beam energy was determined by measuring the recoil electron energy from Compton scattering with a tagging counter which consisted of 2 layers of a combination of a hodoscope and a silicon strip detector. The photon energy resolution was 15 MeV in root-mean-square (RMS). The photon intensity, integrated from 1.5 GeV to 2.4 GeV, was 5×10^5/s. Half of the data was taken with vertically polarized photons and the other half with horizontally polarized photons. A liquid hydrogen target with a thickness of 5.6 cm was used.

Charged hadrons were detected by the LEPS spectrometer covering forward angles. The spectrometer consisted of a plastic-scintillation start counter (SC), a silica-aerogel Čerenkov counter (AC), a silicon vertex detector, a dipole magnet, three multi-wire drift chambers, and a time-of-flight (TOF) wall. The field strength of the dipole magnet was 0.7 T at its center. The angular coverage of the spectrometer was about ±0.4 rad and ±0.2 rad in the horizontal and vertical directions, respectively. The SC determined the trigger timing for the data acquisition system. The AC with a refractive index of 1.03 was used to reject e^+e^- events at the trigger level.

Charged particles were momentum analyzed by using information from the silicon vertex detector and the three drift chambers. Tracks fitted within a 98% confidence level were accepted for further analysis. The TOF measurement was performed by using the RF signal from the 8-GeV electron storage ring as the start timing and signals of 40 plastic scintillators in the TOF wall as the stop timing. The particle mass was determined using the momentum, the path length and the time-of-flight.

After selecting K^+ particles in the spectrometer, the missing mass of the $\gamma p \to K^+X$ reaction was calculated. The left plot in figure 1 shows the missing mass spectrum of K^+ photoproduction. Peaks corresponding to $\Lambda(1116)$, $\Sigma^0(1193)$ and hyperon resonances are observed. In the analysis of π^0 photoproduction, protons were selected and the missing mass of the $\gamma p \to pX$ reaction was obtained to identify π^0 particles. The missing mass spectrum for the $\gamma p \to pX$ reaction is shown in the right plot of figure 1. Peaks due to π^0, η and ω/ρ^0 photoproduction are observed.

The spectrometer acceptance, including the efficiency for detectors and track reconstruction, was obtained using a Monte Carlo simulation with the GEANT3 code. The systematic uncertainty of the target thickness, due to fluctuations of the temperature and pressure of the liquid hydrogen, was esti-

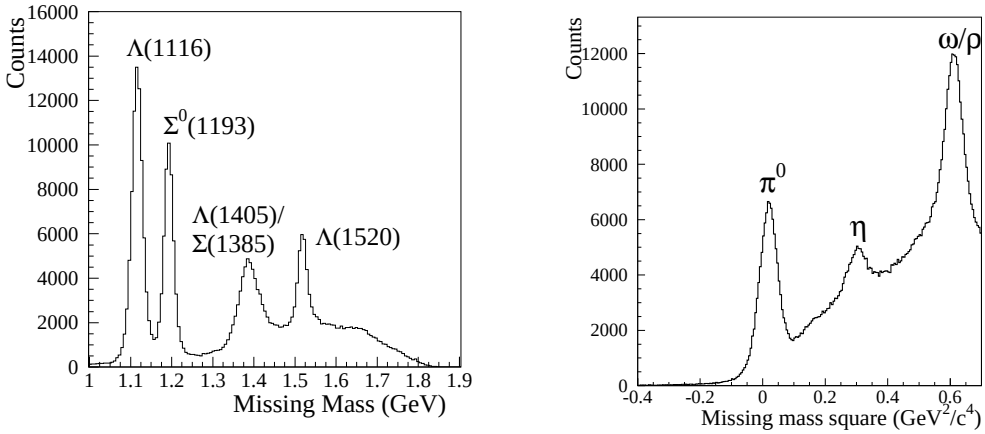

Figure 1: Left; Missing mass of the $\gamma p \to K^+X$ reaction. Right; Missing mass square of the $\gamma p \to pX$ reaction.

mated to be 1.0%. The systematic error of the photon number normalization was 3.0%. The systematic uncertainty of the aerogel Čerenkov counter (AC) due to accidental vetoes and δ-rays was measured to be lower than 1.6%.

3 Results

3.1 K^+ photoproduction

Figure 2 shows the experimental results of the differential cross sections and the photon beam asymmetries as a function of $\cos\Theta_{c.m.}$ for the $K^+\Lambda$ and $K^+\Sigma^0$ reactions. The signs of the photon beam asymmetries for both reactions were found to be positive. The positive sign means that K^+ particles are emitted preferentially in the orthogonal direction to the photon polarization. In both reactions the photon beam asymmetry increases with increasing photon energy and shows an angular distribution flat below $W = 2.0$ GeV. Compared to the $K^+\Lambda$ channel, the photon beam asymmetries for the $K^+\Sigma^0$ channel exhibits a flatter dependence on angle.

The LEPS data of differential cross sections connect smoothly to the CLAS data. It is seen that the $K^+\Lambda$ cross section increases at forward angles while the $K^+\Sigma^0$ cross section decreases except for the low energy regions of $W = 1.947$ and 2.029 GeV. The experimental data for the $K^+\Lambda$ and $K^+\Sigma^0$ reactions are compared with Mart and Bennhold's model calcu-

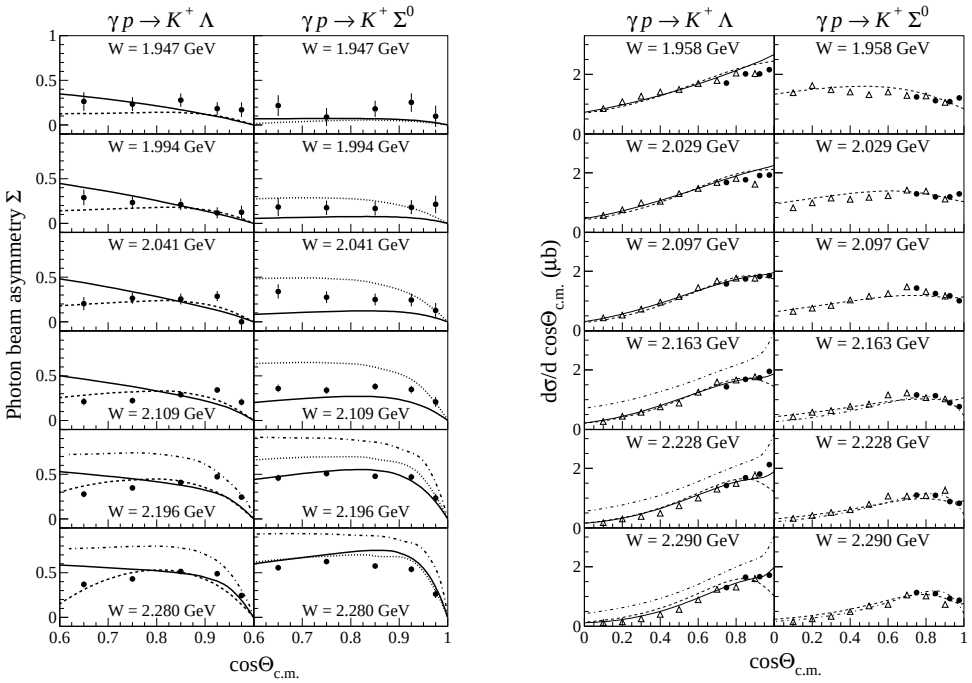

Figure 2: Angular dependence of photon beam asymmetries (left) and differential cross sections (right) for the $\gamma p \to K^+\Lambda$ and $\gamma p \to K^+\Sigma^0$ reactions. Closed circles are LEPS data and open triangles are CLAS data. Dot-dashed, dashed and solid curves are the theoretical calculations with the Regge model, the Feynman diagram and the mixing model of the Regge model and the Feynman diagram, respectively [8].

lation in figure 2. The mixing model calculation agrees with the data for the $K^+\Lambda$ reaction while the calculation of the Feynman diagram only agrees with the data for the $K^+\Sigma^0$ reaction. The calculations of the Feynman diagram increase as the scattering angle becomes smaller, then they drop at $\cos\Theta_{c.m.}$ >0.85 for both reactions. The model calculation without inclusion of Regge amplitudes cannot explain the observed angular distributions for the $K^+\Lambda$ reaction. The Regge model calculation shows steep increase for the $K^+\Lambda$ while it drops for the $K^+\Sigma^0$ at $\cos\Theta_{c.m.}$ >0.9. In the Regge model, the K exchange contribution is large for the $K^+\Lambda$ but is small for the $K^+\Sigma^0$ at forward angles. In the high energy data measured at $W > 3.2$ GeV at SLAC, the $K^+\Lambda$ shows a forward peak but the $K^+\Sigma^0$ does not [9]. This result was discussed in terms of the dominance of the K exchange for the $K^+\Lambda$ [5]. In our data the same feature is seen at $W = 2.1$ to 2.3 GeV.

3.2 π^0 photoproduction

Figure 3 shows differential cross sections as a function of the π^0 scattering angle. The cross sections measured in the present experiment agree mostly with previously published data [10–12]. The data show a backward peaking at $\cos\Theta_{c.m.} < -0.85$ above 1.9 GeV while the data do not show the backward peaking below 1.9 GeV. The backward peaking suggests that the u-channel contribution is not negligibly small. The u-channel nucleon exchange process is expected to produce the backward peaking at high energies.

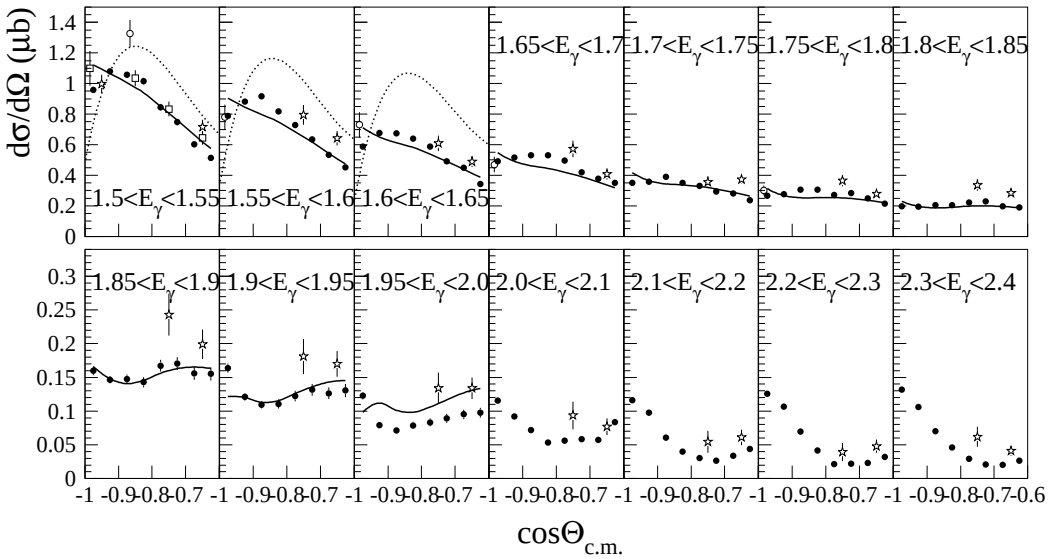

Figure 3: Differential cross sections as a function of the π^0 scattering angle, $\cos\Theta_{c.m.}$. The closed circles are the results of the present analysis. Only statistical errors are plotted. Most of them are smaller than the size of symbols. The open squares, open stars and open circles are the GRAAL data [10], the ELSA data [11], and the Bonn data in 1979 [12], respectively. The solid and dotted curves are the results of the SAID [13] and the MAID2007 [14], respectively.

The LEPS data mostly agree with the SAID results. A small enhancement structure appears around $\cos\Theta_{c.m.} = -0.7$ at $E_\gamma = 1.85$–1.95 GeV in the LEPS data which have not been clearly observed in the previous data due to the poor statistics. The enhancement is well reproduced by the SAID analysis. However, the SAID calculations do not reproduce the backward

peaking at E_γ = 1.9–2.0 GeV. The MAID2007 results overestimate the data at cos$\Theta_{c.m.}$ > –0.9 and underestimate the data at the most backward angles. The discrepancy becomes larger as the photon energy goes higher. Further improvement of the theoretical calculations will be expected at higher energies and backward angles by including the present data.

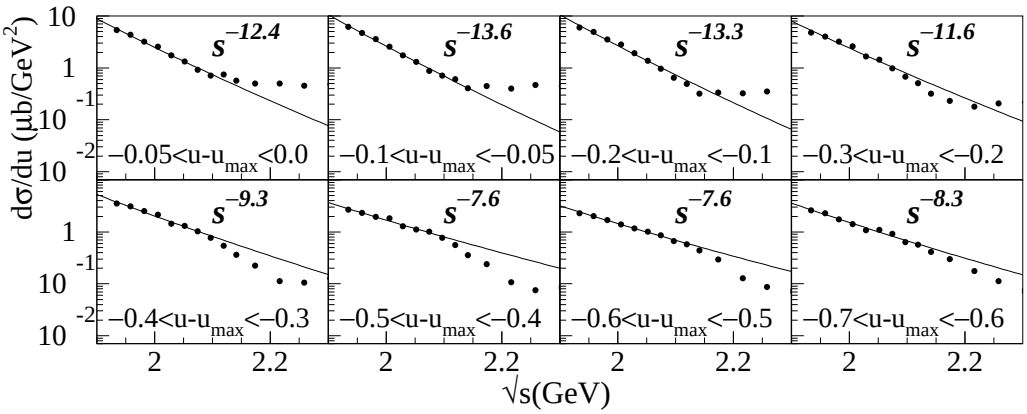

Figure 4: Differential cross sections as a function of the total energy, $\sqrt{s}$, for the $\gamma p \rightarrow \pi^0 p$ reaction. The closed circles are the results of the present analysis. The curves are the fitting results of As^{-x} for the data at $\sqrt{s}$ <2.1 GeV, where A and x are fitting parameters [4].

Figure 4 shows differential cross sections as a function of the total energy, $\sqrt{s}$ at eight bins of $u - u_{\rm max}$ [GeV^2]. The maximum value, $u_{\rm max}$, occurs when the proton goes forward at 0° from the photon beam direction. The energy-dependent slope of the cross sections for π^0 production has been determined for the first time in this energy region. The curves are the results of fitting the data from $\sqrt{s}$ = 1.93 GeV (the lowest energy) to 2.1 GeV using a function of As^{-x}. The slope parameter, x, obtained from the fitting is indicated in each plot.

The slope parameter, x, becomes smaller at larger $\mid u - u_{\rm max} \mid$. The LEPS photon energy sits in the transition region from nucleon-meson degrees of freedom to quark-gluon degrees of freedom. The cross sections are known to approximately follow the constituent counting rules above the resonance region and at large scattering angles [15]. If the scaling starts in this photon energy region, the data should follow the counting rule, s^{2-n}. The quantity n is the total number of interacting photon and quarks. The value n is 9 for

π^0 photoproduction. The data becomes closer to the scaling behavior, s^{-7}, at the larger $\mid u - u_{\max} \mid$ where the momentum transfer is large. Although the LEPS photon energy is slightly lower than the onset of scaling, the LEPS data provide information on the early onset of scaling.

The differential cross sections sharply decrease for $\sqrt{s}$ below 2.1 GeV. Above 2.1 GeV, the cross sections do not agree with the fitting curves determined by the data at lower $\sqrt{s}$. In order to explain the current data in the u channel kinematics, new mechanisms would be necessary.

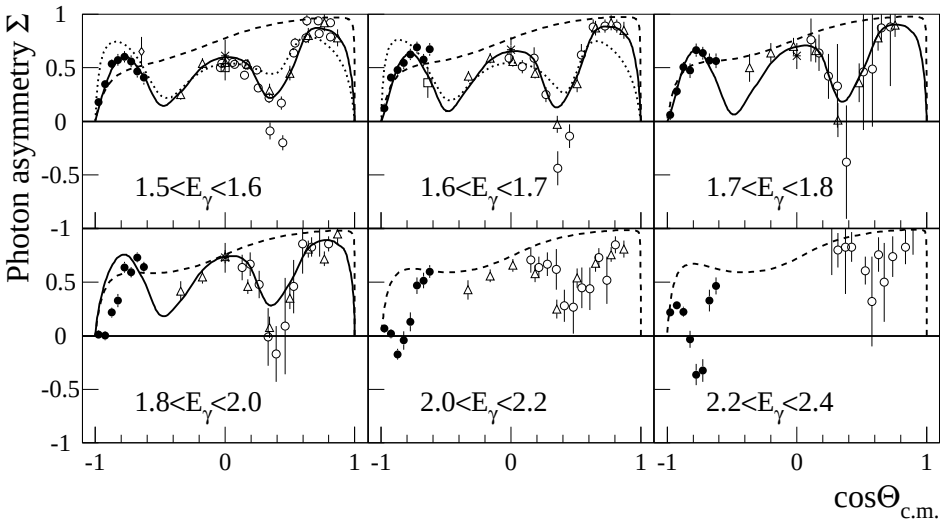

Figure 5: Photon beam asymmetries Σ as a function of the π^0 scattering angle, $\cos\Theta_{c.m.}$. The closed circles are the results of the present analysis. The other plots are the data from other facilities, $\square$ [16], $\triangle$ [17], $\circ$ [18], $*$ [19]. The solid and dotted curves are the SAID results [13] and the MAID2007 results [14], respectively. The dashed curves are the calculations of the Born (non-resonant) term by the SL model [20].

The photon beam asymmetry is sensitive to the interference of different diagrams. Resonances can be studied from the photon beam asymmetry combined with cross section data. Figure 5 shows the photon beam asymmetries. The photon asymmetries indicate a bump structure around $\cos\Theta_{c.m.} = -0.8$ at $E_\gamma < 1.8$ GeV. Two bumps are observed around $\cos\Theta_{c.m.} = 0$ and 0.75 in the data from other facilities. A similar angular distribution of the photon

asymmetries has been obtained at $E_\gamma < 1.5$ GeV by the GRAAL collaboration [10]. The MAID2007 calculation including 13 resonances reproduces these bump structures. The SAID calculation agrees with the photon beam asymmetry data, and reproduces the bump structures up to $E_\gamma = 1.8$ GeV, even though the LEPS data are not used for a fit in the analysis. Therefore, below 1.8 GeV, the LEPS data are explained by the well-known resonances.

The angular distribution changes above $E_\gamma = 1.8$ GeV as well as the differential cross sections. A strong angular dependence appears at $E_\gamma >$ 2.0 GeV; The photon asymmetries show a dip structure around $\cos\Theta_{c.m.} =$ –0.8, and the data drop to a negative sign, and then rise up to a positive sign. The discrepancy between the LEPS data and the SAID results becomes large at $E_\gamma = 1.8$–2.0 GeV. The SL model with the Born terms only shows a positive sign and does not reproduce the dip structure. To explain this strong angular dependence, new mechanism or new resonances are required. There are some candidates of resonances above 2.0 GeV.

4 Summary

K^+ photoproduction and π^0 photoproduction have been studied by using linearly polarized photons at the SPring-8/LEPS facility with 1.5–2.4 GeV. Differential cross sections and photon beam asymmetries have been measured. The differential cross sections for the $\gamma p \to K^+\Lambda$ reaction rise at forward angles while the cross sections for the $\gamma p \to K^+\Sigma^0$ reaction drop. The exchanged meson in t-channel will be studied using the LEPS data at forward angles.

The differential cross sections for π^0 photoproduction at $E_\gamma > 1.9$ GeV show a backward peaking. It is suggested that the u-channel contribution is important. In addition, photon beam asymmetries have been obtained. Above 2.0 GeV, a strong angular distribution is found around $\cos\Theta_{c.m.} = -0.8$. In order to explain this structure, the presence of new high-mass resonances combined with the u-channel diagrams is required.

5 References

References

[1] Particle Data Group, http://pdg.lbl.gov.

[2] S. Capstick and W. Roberts, *Phys. Rev.* **D49**, 4570 (1994);
S. Capstick and W. Roberts, *Phys. Rev.* **D58**, 074011 (1998).

[3] D. Dutta, H. Gao, T.-S. H. Lee, *Phys. Rev.* **C65**, 044619 (2002).

[4] R.W. Clifft, *et al.*, *Phys. Lett.* **B72**, 144 (1977).

[5] M. Guidal, M. Laget, M. Vanderhaeghen, *Nucl. Phys.* **A627**, 645 (1997).

[6] T. Nakano, *Nucl. Phys.* **A721**, 112c (2003).

[7] R.G.T. Zegers, M. Sumihama, *et al., Phys. Rev. Lett.* **91**, 092001 (2003); M. Sumihama, *et al., Phys. Rev.* **C73** 035214 (2006).

[8] T. Mart and C. Bennhold, 'Kaon photoproduction in the Feynman and Regge theories,' arXiv:nucl-th/0412097.

[9] A.M. Boyarski, F. Bulos, W. Busza, R. Diebold, S.D. Ecklund, G.E. Fischer, Y. Murata, J.R. Rees, B. Richter, and W.S. C. Williams, *Phys. Rev. Lett.* **22**, 1131 (1969).

[10] O. Bartalini, *et al., Eur. Phys. J.* **A26**, 399 (2005).

[11] O. Bartholomy, *et al., Phys. Rev. Lett.* **94**, 012503 (2005).

[12] K.H. Althoff, *et al., Z. Phys.* **C1**, 327 (1979).

[13] R. Arndt, W. J. Briscoe, I. I. Strakovsky, R. L. Workman, *Phys. Rev.* **C66**, 055213 (2002);
http://gwdac.phys.gwu.edu/.

[14] L. Tiator, S. Kamalov, Proceedings of NSTAR2005, nucl-th/0603012;
D. Drechsel, O. Hanstein, S.S. Kamalov, L. Tiator, *Nucl. Phys.* **A645** 145 (1999);
http://www.kph.uni-mainz.de/MAID/maid2007/.

[15] S.J. Brodsky, G.R. Farrar, *Phys. Rev. Lett.* **31**, 1153 (1973).

[16] L.O. Abrahamian, *et al., Phys. Lett.* **B48**, 463 (1974).

[17] P.J. Bussey, *et al., Nucl. Phys.* **B154**, 492 (1979).

[18] P.J. Bussey, *et al., Nucl. Phys.* **B104**, 253 (1976).

[19] J. Alspector, *et al., Phys. Rev. Lett.* **28**, 140. (1972)

[20] T. Sato, T.-S. H. Lee, *Phys. Rev.* **C54**, 2660 (1996);
T. Sato, T.-S. H. Lee, *Phys. Rev.* **C63**, 055201 (2001).